FEBS Letters 580 (2006) 2451–2457

Cytotoxicity of albebetin oligomers depends on cross-β-sheet formation

Vladimir Zamotin[a], Anna Gharibyan[a], Natalia V. Gibanova[b], Marika A. Lavrikova[b], Dmitry A. Dolgikh[b], Michail P. Kirpichnikov[b], Irina A. Kostanyan[b], Ludmilla A. Morozova-Roche[a,*]

[a] *Department of Medical Biochemistry and Biophysics, Umeå University, SE-901 87 Umeå, Sweden*
[b] *Shemyakin & Ovchinnikov Institute of Bioorganic Chemistry, Russian Academy of Sciences, Moscow, Russia*

Received 24 February 2006; revised 16 March 2006; accepted 21 March 2006

Available online 7 April 2006

Edited by Jesus Avila

Abstract Prefibrillar cytotoxicity was suggested as a common amyloid characteristic. We showed two types of albebetin prefibrillar oligomers are formed during incubation at pH 7.3. Initial round-shaped oligomers consist of 10–15 molecules determined by atomic force microscopy, do not bind thioflavin-T and do not affect viability of granular neurons and SH-SY5Y cells. They are converted into ca. 30–40-mers possessing cross-β-sheet and reducing viability of neuronal cells. Neither monomers nor fibrils possess cytotoxicity. We suggest that oligomeric size is important for stabilising cross-β-sheet core critical for cytotoxicity. As albebetin was used as a carrier-protein for drug delivery, examination of amyloidogenicity is required prior polypeptide biomedical applications.

Keywords: Amyloid; Oligomers; Cytotoxicity; Atomic force microscopy

1. Introduction

It is widely accepted that aggregated forms associated with amyloid diseases are critically involved in cellular toxicity and tissue damage. However the definition of the toxic amyloid species and their particular structural properties exerting the specific cytotoxic effect remain controversial. In the last years a number of studies have supported the hypothesis that early aggregates or prefibrillar species are implicated in cytotoxicity while fibrillar amyloid deposits serve as an escape route for smaller aggregates [1–5]. Among them Kayed et al. observed that intermediate-size water soluble oligomers of $A\beta_{1-40}$ and other five proteins form sheared structures characterized by similar conformational epitope, suggesting that they exert cytotoxicity via similar mechanisms [6]. The finding that disease non-related proteins SH3 domain and HypF can form transient toxic amyloid oligomers led to suggestion that amyloid toxicity is a generic phenomenon which can be attributed to many naturally occurring proteins [7]. Recently reported cytotoxicity of transient amyloid oligomers of lysozyme is particularly important as it is a naturally abundant protein present in a variety of organisms and food products indicating that amyloid toxicity occurs under variety of conditions in our daily life [8].

Currently, a broad range of structures are considered to be cytotoxic including misfolded monomer and hexamer of transthyretin [9], 8–9 nm globular structures of transthyretin mutants [2], 8 to 20-mers of equine lysozyme [8], 4–200 nm diameter granules of PI3-SH3 domain and short aggregates of 4–8 nm width of HypF [10], 3–5 nm spherical aggregates of α-synuclein [11,12], 90 kDa oligomers of $A\beta_{1-42}$ [13] and others. Even the process of nucleation dependent polymerization of $A\beta_{1-40}$ itself was suggested to be a primarily cause of cytotoxicity [14]. As amyloid structures formed of many proteins have been found to be also highly heterogeneous within the same specimen and largely affected by environmental conditions and history of the sample, this hampers the clear description of toxic species [3,15,16].

In our studies we have focused on characterization of the amyloid cytotoxicity of de novo protein albebetin. Albebetin was engineered as a protein with pre-determined 3D structure [17] and it was used as an inert carrier matrix for drug delivery [18–20]. It is a 73 amino acid residue protein composed of two sets of αββ motives forming four stranded β-sheet covered by two α-helices and characterized by a mobile molten globule type conformation at neutral pH. The compactness of this molecule is achieved due to short loops connecting the secondary structure elements. In our previous studies we have shown that albebetin readily assembles into a variety of amyloid structures during its incubation under physiological conditions [21]. Here we examine the cytotoxic properties of main amyloid species of albebetin relating their structural properties with exerted cytotoxicity. The advantage of using albebetin as a structural model for cytotoxicity studies lies in its ability to convert into amyloid under conditions closely resembling those of the cytotoxicity assays and therefore little perturbation of toxic species occurs in the course of the experiment. Taking into account that albebetin is a possible drug delivery agent, examination of its cytotoxic properties is also important for its potential biomedical applications.

2. Materials and methods

2.1. Protein samples

Albebetin was expressed in *Escherichia coli* and purified as described previously [18]. Its concentration was determined by using Bradford assay. In order to produce amyloid structures albebetin

*Corresponding author. Fax: +46 90 786 97 95.
E-mail address: Ludmilla.Morozova-Roche@medchem.umu.se (L.A. Morozova-Roche).

Abbreviations: AFM, atomic force microscopy; CD, circular dichroism; SPIP, scanning probe image processor

0014-5793/$32.00 © 2006 Published by Elsevier B.V. on behalf of the Federation of European Biochemical Societies.
doi:10.1016/j.febslet.2006.03.074

was incubated at a concentration of 1.2 mM in 20 mM HEPES buffer, 50 mM NaCl, 0.2% sodium azide, pH 7.4. $A\beta_{25-35}$ and cell apoptotic agent D-sphingosine were purchased from Sigma (USA). $A\beta_{25-35}$ amyloid was produced upon 3 days of incubation at the same conditions as albebetin.

2.2. Spectroscopic characterisation of amyloid formation

Thioflavine-T binding amyloid assay was carried out by using a modification of the method of Levine [22]. Fluorescence measurements were performed on a Jasco spectrofluorometer FP 6500 (Japan) with excitation at 440 nm and emission collected between 450 and 550 nm, setting the excitation and emission slits at 5 nm.

Congo red binding assay was performed according to the procedure described in [23]. Optical absorbance spectra were recorded on a NanoDrop ND-1000 spectrophotometer (USA).

Far UV circular dichroism (CD) spectra were collected on a Jasco J720 CD UV spectrometer (Japan) equipped with a water bath temperature controller using a 1 mm light path quartz cell.

2.3. Neuronal cells

Cerebellar granular neurons were extracted from cerebellum of 8 days aged male Wistar rats. Cerebellum tissues were incubated in Krebs-Ringer solution (120 mM NaCl, 4.8 mM KCl, 1.2 mM KH_2PO_4, 25 mM $NaHCO_3$, 14 mM glucose, 0.3% BSA) with 0.25% trypsin. Cells were suspended in the same solution in the presence of 0.1% DNAse and 0.05% trypsin inhibitor, centrifuged and resuspended in BME medium containing 10% calf fetal serum and 25 mM KCl. Cell suspensions with the density of 1.5×10^6 cell/ml were cultivated in 24 well plates in 5% CO_2 at 37 °C. After 24 h the cell proliferation was stopped by adding 10 μM arabinosylcytosine (Sigma, USA) On 7–8 days of cultivation the culture medium was changed to BME with 3% calf fetal serum and cells were subjected to the viability tests.

SH-SY5Y neuroblastoma cells were cultured in Dulbecco's modified Eagle's medium supplemented with 10% FBS and antibiotics in a 5% CO_2 humidified atmosphere at 37 °C.

2.4. Mitochondrial activity assay

Cells were plated at a density of 10 000 cells per well in 96-well plates. The aliquots of amyloid samples were added to the wells (100 μl) and cerebellar granular neurons were incubated for 16 h, while SH-SY5Y cells for 24 h, respectively. 10 μl of MTT (3-(4,5-dimethylthiazol-2-yl)-2,5-diphenyltetrazolium bromide) labelling reagent (Roche Applied Sciences, Germany) was added to cerebellar granular neurons and tetrazolium salt WST-1 (4-[3-(4-iodophenyl)-2-(4-nitrophenyl)-2H-5-tetrazolio]-1,3-benzene disulfonate) (Roche Applied Sciences, Germany) to SH-SY5Y cells, respectively. The samples were incubated for further 4 h. 100 μl of solubilization mixture (10% SDS, 0.01 M HCl) was added to each well and the samples were incubated overnight. Absorbance of formazan at 570 nm was measured with an ELISA plate reader (Labsystems, USA).

2.5. Atomic force microscopy

Atomic force microscopy (AFM) measurements were performed on a PICO SPM microscope (Molecular Imaging, USA) in a tapping mode using a 100 nm scanner with acoustically driven cantilevers. Cantilevers carried etched silicon probes of TESP model with diameter of 10 nm and less (Digital Instruments, USA) were operated at resonance frequencies in 170–190 or 320–370 kHz range. Scanning resolution was 512×512 pixels. Height, amplitude and phase data were collected simultaneously. The scanning was performed in trace and retrace to avoid the scan artefacts. Images were flattened and plane adjusted. Before imaging, the scanner was calibrated by using a standard 1 nm calibration grid (Molecular Imaging, USA) in the x–y plane and measuring atomic steps on a highly oriented pyrolytic graphite surface in the z-axis. For ambient imaging, amyloid samples were prepared as described previously [21].

2.6. Measurements of particle dimensions

The dimensions of individual particles were measured in multiple cross-sections of AFM height images by using PicoPlus software (Molecular Imaging, USA). The distribution of z-heights of all particles adhered from the sample to the mica surface was evaluated by the grain analysis module of scanning probe image processor (SPIP) software (Image Metrology, Denmark). In each sample we have analyzed by the SPIP grain module 3–4 mica areas of 1.5×1.5 μm size with 4000–8000 particles in each.

The volume of the oligomeric particle was calculated by equation [24,25] where d is the diameter of the particle approximated as spherical cup and measured at its half height, h

$$V_{\mathrm{AFM}} = \pi h d^2/8. \quad (1)$$

The molecular volume of monomeric albebetin was estimated using equation

$$V_{\mathrm{m}} = (M_0/N_0)(V_1 + pV_2), \quad (2)$$

where M_0 is the protein molecular weight, N_0 is Avogadro's number, p is the extent of protein hydration (0.4 mol H_2O/mol protein), and V_1 and V_2 are the partial specific volumes of protein (0.74 $cm^3\ g^{-1}$) and water (1 $cm^3\ g^{-1}$) molecules, respectively [24,25]. The number of albebetin monomers in oligomers was determined by the ratio:

$$n = V_{\mathrm{AFM}}/V_{\mathrm{m}}. \quad (3)$$

To evaluate the accuracy of our measurements, we used the reference samples such as spherical latex particles with circa 1.5 nm diameter and single wall carbon nanotubes with circa 1 nm diameter as well as applied the tip deconvolution module of the SPIP software (Image Metrology, Denmark) accounting for the geometry of the tips. Measurements of the reference samples confirmed the conclusion of [8,24,25], that a spherical cap approximation sufficiently describes protein particles. Processing images with the SPIP tip deconvolution module indicated that the shape of the tip did not produce topological distortions.

2.7. Statistical analysis

Statistical analysis of cell viability measurements was performed by Student's paired t test. Results are expressed as mean ± S.D. $P < 0.05$ was considered statistically significant.

3. Results

3.1. Spectroscopic characterisation of cross-β-sheet containing amyloid

The fibrillation of albebetin proceeds within hours of incubation at physiological pH and 57 °C. The overall kinetics was monitored by thioflavine T fluorescence assay as this dye has a propensity to bind to cross-β-sheet containing amyloid [22,23]. The results are shown in Fig. 1, indicating that after a short lag-phase of ca. 2 h the development of cross-β-sheet structure takes place in amyloid aggregates which results in significant enhancement of thioflavine T dye fluorescence. The thioflavine T fluorescence increases by 4–5 fold at the plateau level reached after ca. 15 h and remained in this range upon further incubation up till weeks (data not shown).

In addition, ABB fibrillation was characterized by Congo red assay as this dye is also specifically binds to amyloid structures; the results are shown in Fig. 1B. Freshly dissolved protein and the oligomers formed during the lag phase in the kinetic do not bind Congo red, which does not affect the position of the dye absorbance spectra. The binding of Congo red by the oligomers formed after 6 h of incubation and by fibrils assembled after 24 h leads to the red shift of Congo red absorbance by 9 and 17 nm, respectively.

In order to characterise the changes of the secondary structure during amyloid assembly the far UV CD spectra were recorded as shown in Fig. 1C. Due to a high degree of conformational flexibility of albebetin the spectra of freshly dissolved protein as well as of the sample incubated for 2 h are characterized by a pronounced signal at 205–210 nm corresponding to random-coil. The formation of the later oligomers

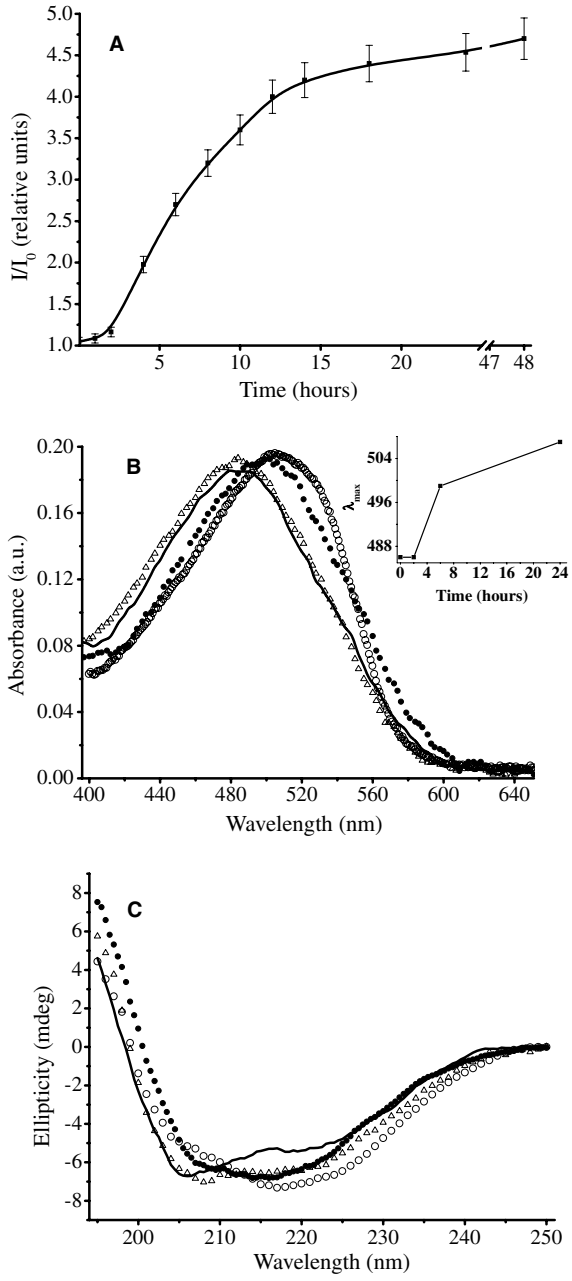

Fig. 1. Albebetin fibrillation monitored by spectroscopic techniques. Protein was incubated at pH 7.3 and 57 °C (see Section 2). (A) Thioflavin T binding to albebetin amyloid. I/I_0 is a relative fluorescence of thioflavin T, where I refers to the dye bound to amyloid and I_0 to free dye in solution. (B) Congo red binding to albebetin amyloid. Congo red spectrum in the presence of freshly dissolved protein is denoted by black line, in the presence of the 2 h sample by open triangles, the 6 h sample – by filled circles and the 24 h sample – by open circles. Insertion shows the long wavelength shift of the spectra of Congo red dye bound to amyloid during its incubation. (C) Far UV CD spectra of albebetin amyloid. The spectra are denoted as (B).

(6 h) and fibrils (24 h of incubation), by contrast, is manifested in significant changes of the shape of the far-UV CD spectra in which the minimum at 216–220 nm become more pronounced revealing a substantial increase of the β-sheet content (Fig. 1C). Due to heterogeneity of the sample and the presence of the residual amount of monomeric albebetin even after 24 h of incubation, the CD signal deviates from the classical β-sheet CD spectrum indicating the presence of some other types of secondary structure.

3.2. AFM imaging of amyloid oligomers and fibrils

The molecular species corresponding to the lag- (2 h), growth-phases (6 h) as well as to the plateau level (24 and 48 h) of incubation (Fig. 1) were subjected to detail AFM analysis. Their AFM images are presented in Fig. 2. In the first two samples oligomers were dominant species. There were also some non-structured aggregates in both samples; similar aggregates were also observed in freshly dissolved protein and among mature fibrils. After 6 h of incubation the fibrils have not yet been observed, even in a small number. The plateau of the kinetics corresponds to the formation of fibrillar species. After 24 h of incubation the fibrils were characterized by 1.5 nm height in the AFM cross-sections, which is a characteristic dimension of single protofilaments [15]; their length varied from ca. 10 to ca. 500 nm. On 48 h of incubation the fibrils have matured; they significantly thickened due to lateral assembly of protofilaments, their widths varied from 2–3 up to 10–15 nm and their lengths grew to a few microns.

The dimensions of oligomeric species shown in Fig. 2A and B were analyzed by both manual AFM cross-sections of the individual particles and by measuring of all particles within the AFM imaging field with the grain analysis SPIP program. The distributions of the particle heights are presented in Fig. 3. Both techniques of height measurements showed consistent results (compare Fig. 3A and B with the corresponding insertions). The distribution after 2 h of incubation (Fig. 3A) is centred at 0.8–1.0 nm with the diameter measured at half-height of 20 ± 5 nm. These species are composed of ca. 10–15 monomers estimated by Eqs. (1)–(3).

The major population of species after 6-h incubation (Fig. 3B) is characterized by 1.6–2.2 nm heights with the diameter at half-height of 30 ± 5 nm. These oligomers are comprised of 25–40 molecules estimated as described above. Similar oligomers are also observed after 12 h of incubation corresponding to the kinetic growth phase (Fig. 1). Both oligomeric size distributions are broad reflecting heterogeneity of amyloid samples that was confirmed by native gel electrophoresis demonstrating the ladder of oligomeric species in both cases (data not shown). The stability of the oligomers was assessed after 24 h incubation in the culture medium corresponding to the cytotoxicity tests; measurements of their dimensions by grain analysis SPIP module showed the same distributions.

3.3. Effect of amyloid on cell viability

The aliquots containing amyloid structures of albebetin were added to two cell types, cerebellar granular neurons and SH-SY5Y cells. Cell survival in the presence of amyloid was assessed by the ability of mitochondrial dehydrogenases to reduce tetrazolium salt in viable cells. The results are presented in Fig. 4. In control measurements we have shown that there was no difference in the viability of untreated cells and cells with added buffer used for amyloid incubation. $A\beta_{25-35}$ amyloid structures and apoptotic agent D-sphingosine were used as positive controls of induced cytotoxicity. Upon addition of $A\beta_{25-35}$ amyloid the survival of granular neurons decreased by ca. 45% (Fig. 4A). Similar effect was observed with SH-

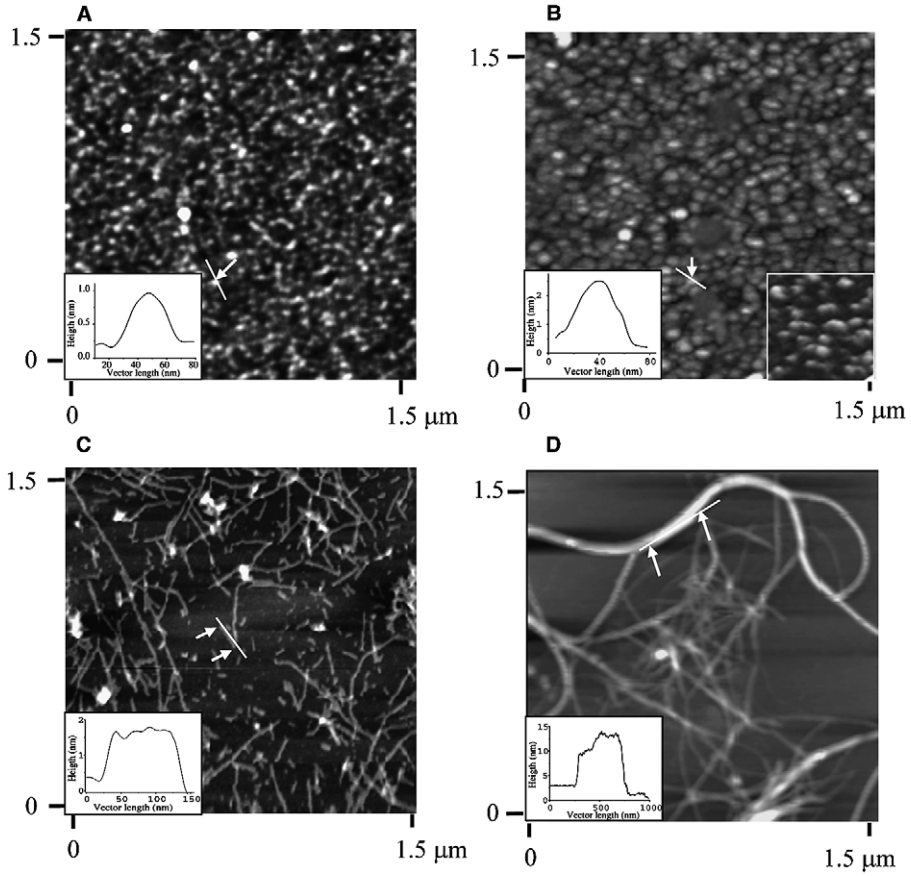

Fig. 2. AFM imaging of albebetin amyloidogenesis. Amyloid samples after 2 h (A) and 6 h (B) incubation (see Section 2) containing oligomers; after 24 h (C) and 48 h (D) containing protofilaments and mature fibrils, respectively. Cross-sections of individual species are shown by white arrows. Insertions in the left lower corners in each figure show the corresponding cross-sections. The right lower corner insertion in (B) shows three-dimensional image of spherical oligomers. *z*-scale is 3 nm in (A), 5 nm in (B), 10 nm in (C) and 20 nm in (D).

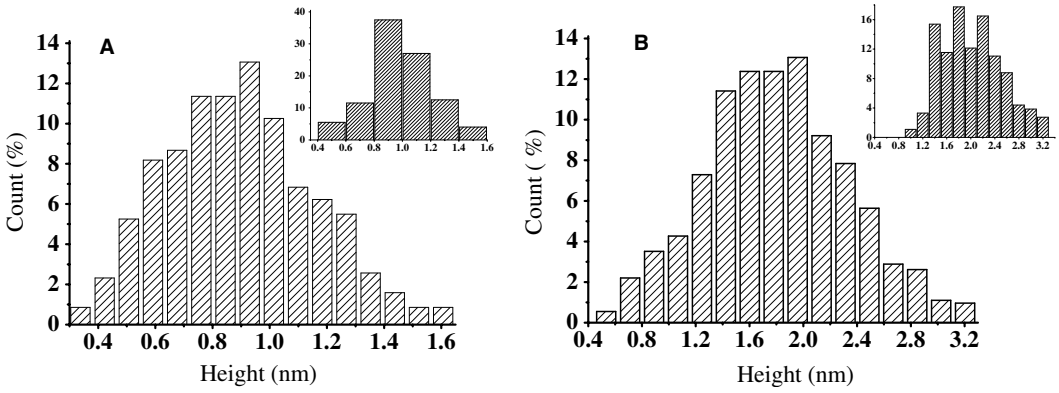

Fig. 3. Distributions of *z*-heights of albebetin oligomers. The sample of albebetin after 2 h (A) and 6 h (B) of incubation (see Section 2). Measurements were carried out by using SPIP software. Insertions in both figures show the distributions measured by manual cross-section analysis. Counts of grains are shown in percentage.

SY5Y cells in the presence of D-sphingosine (Fig. 4B). Monomeric albebetin and the samples containing smaller 10–15-mers oligomers did not affect cell viability. By contrast, the larger 25–40-mers oligomers produced the cytotoxic effect. The cell viability depends on the concentration of added amyloid (Fig. 4). The viability of granular neurons decreases by 25–30% and SH-SY5Y by ca. 15% in the presence of 50 μM aliquot of amyloid oligomers. Amyloid protofilaments and fibrils shown in Fig. 2C and D did not produce the cytotoxic effect on SH-SY5Y cells, however we observed small but statistically significant ($P < 0.01$) decrease of viability by ca. 5% in granular neuronal culture.

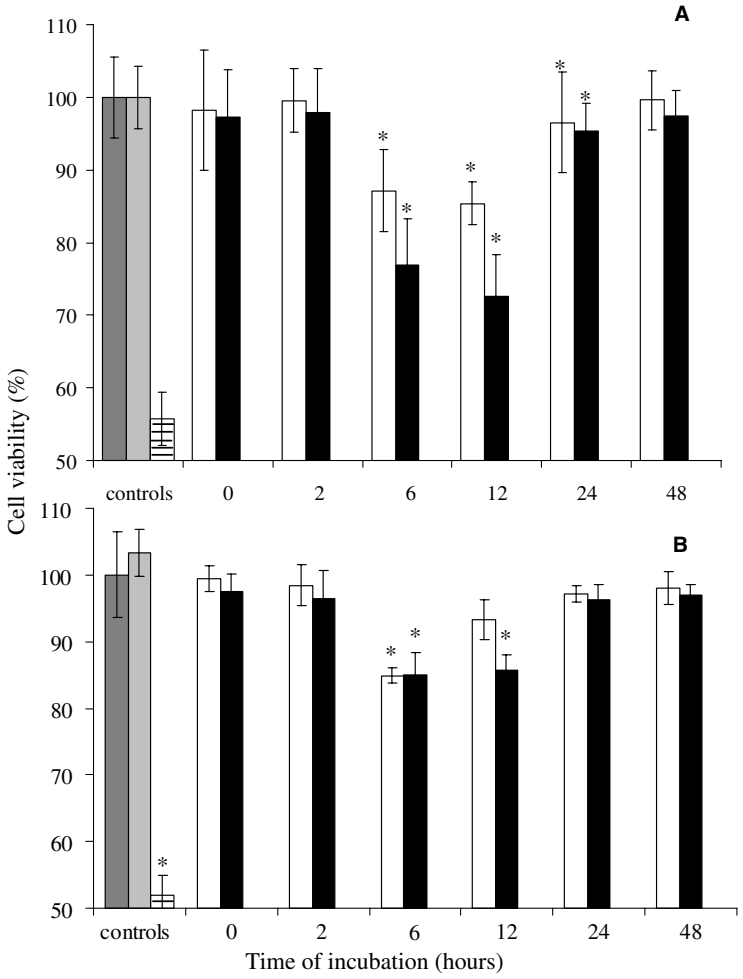

Fig. 4. Effect of albebetin amyloid on viability of cerebellar granular neurons (A) and SH-SY5Y neuroblastoma cells (B). Time of incubation of albebetin amyloid is shown along *x*-axis. White bars correspond to addition of 5 μM albebetin solution and black bars to 50 μM. Control measurements of the viability of unperturbed cells are shown in dark grey, in the presence of aliquot of buffer – in light grey, in the presence of $A\beta_{25-35}$ (A) and D-sphingosine (B) – in sparse. $^{*}P < 0.01$.

4. Discussion

Fibrillation process of albebetin, shown to be in a molten globule conformation under neutral pH [17–20], involves the formation of multiple amyloid species, among which at least two types of oligomers can be identified. The first ones are 10–15-mers assembled during the lag phase of incubation. The lack of thioflavine T and Congo red dye binding and the shape of the far UV CD spectrum indicate that cross-β-sheet structure has not yet been developed. The similarity of the far UV CD spectra of monomeric albebetin and the early oligomers indicates that the latter are most likely comprised of molten globule albebetin (Fig. 1C). This type can be referred to pivotal oligomers described previously [21] which either undergo conversion into the larger aggregates or coexist with fibrils. The second type includes oligomers of 25–40-mers size; their binding to amyloid specific dyes thioflavine T and Congo red and the development of far UV CD spectrum similar to the fibrillar CD signal indicate the formation of cross-β-sheet structure. Both types of oligomers exhibit similar round-shaped morphology in AFM images which is commonly associated with prefibrillar amyloid [1–5]. Here we have demonstrated that only the second enlarged type of oligomers produce cytotoxic effect on two kinds of neuronal cells. The current observations of exerted amyloid cytotoxicity by albebetin amyloid are schematically summarized in Fig. 5. Residual cytotoxic effect noticed during the early fibrillation stage (Fig. 4) can be either due to non-specific mechanical damage of the cells by fibrils or can be associated with some remaining fraction of toxic oligomeric species.

The fibrillation of albebetin is consistent with the nucleation conformational conversion model of amyloid formation, in which less structured oligomers are converted into the amyloid competent type consequently assembling into fibrils [26–28]. This is in contrast to the nucleation model in which primary nuclei serve as templates initiating rapid amyloid polymerization [29]. Hierarchy of oligomers undergoing consequent structural conversion with fibril formation at the end has been observed for some other proteins [30,31].

In a light of hypothesis that amyloid acts via common cytotoxic mechanisms [6] it is of crucial importance to provide clear structural description of cytotoxic oligomeric species discriminating them from non-toxic amyloid oligomeric precursors. While the soluble oligomers from different proteins are clearly varied significantly in their size, our results support the view that the development of cross-β-sheet core is essential for

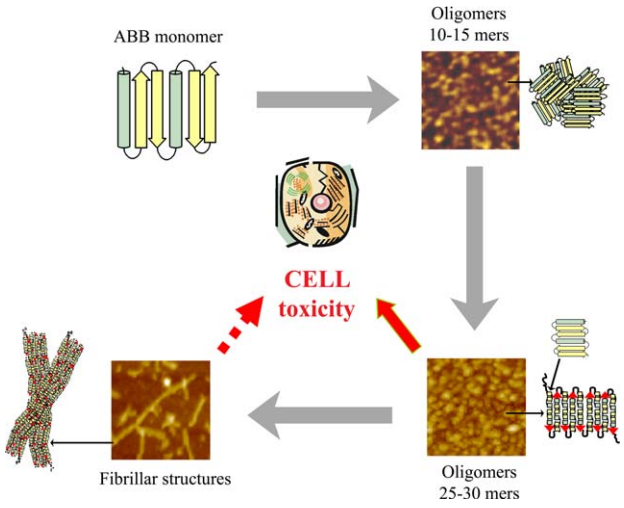

Fig. 5. Schematic presentation of albebetin amyloid pathways and exerted cytotoxicity. Grey arrows show the pathways of amyloid assembly, red ones – cytotoxic effect on cells produced by amyloid. Insertions show AFM images of amyloid structures which are also presented schematically. Albebetin fold is shown by yellow arrows and green columns corresponding to β-strands and α-helices, respectively.

exerted cytotoxicity. Indeed, cross-β-sheet structure is critical both for the interaction of amyloid with cellular receptors [32] and lipid membranes [11,33] implicated in cytotoxicity. The size or stoichiometry of oligomers can be a secondary factor depending on the particular polypeptide sequence though critical for the stabilising the cross-β-sheet structure within the molecular assembly.

Acknowledgements: The financial supports provided by Swedish Medical Research Council, Swedish Royal Academy of Sciences and RAS program on molecular and cellular biology are gratefully acknowledged.

References

[1] Bhatia, R., Lin, H. and Lal, R. (2000) Fresh and globular amyloid beta protein (1–42) induces rapid cellular degeneration: evidence for AβP channel-mediated cellular toxicity. FASEB J. 14, 1233–1243.
[2] Andersson, K., Olofsson, A., Nielsen, E.H., Svehag, S.E. and Lundgren, E. (2002) Only amyloidogenic intermediates of transthyretin induce apoptosis. Biochem. Biophys. Res. Commun. 294, 309–314.
[3] Chromy, B.A., Nowak, R.J., Lambert, M.P., Viola, K.L., Chang, L., Velasco, P.T., Jones, B.W., Fernandez, S.J., Lacor, P.N., Horowitz, P., Finch, C.E., Krafft, G.A. and Klein, W.L. (2003) Self-assembly of $A\beta_{1-42}$ into globular neurotoxins. Biochemistry 11, 12749–12760.
[4] Sirangelo, I., Malmo, C., Iannuzzi, C., Mezzogiorno, A., Bianco, M.R., Papa, M. and Irace, G. (2004) Fibrillogenesis and cytotoxic activity of the amyloid-forming apomyoglobin mutant W7FW14F. J. Biol. Chem. 279, 13183–13189.
[5] Anderluh, G., Gutierrez-Aguirre, I., Rabzelj, S., Ceru, S., Kopitar-Jerala, N., Macek, P., Turk, V. and Zerovnik, E. (2005) Interaction of human stefin B in the prefibrillar oligomeric form with membranes. Correlation with cellular toxicity. FEBS J. 272, 3042–3051.
[6] Kayed, R., Head, E., Thompson, J.L., McIntire, T.M., Milton, S.C., Cotman, C.W. and Glabe, C.G. (2003) Common structure of soluble amyloid oligomers implies common mechanism of pathogenesis. Science 300, 486–489.
[7] Bucciantini, M., Calloni, G., Chiti, F., Formigli, L., Nosi, D., Dobson, C.M. and Stefani, M. (2004) Prefibrillar amyloid protein aggregates share common features of cytotoxicity. J. Biol. Chem. 279, 31374–31382.
[8] Malisauskas, M., Ostman, J., Darinskas, A., Zamotin, V., Liutkevicius, E., Lundgren, E. and Morozova-Roche, L.A. (2005) Does the cytotoxic effect of transient amyloid oligomers from common equine lysozyme in vitro imply innate amyloid toxicity? J. Biol. Chem. 280, 6269–6275.
[9] Reixach, N., Deechongkit, S., Jiang, X., Kelly, J.W. and Buxbaum, J.N. (2004) Tissue damage in the amyloidoses: transthyretin monomers and nonnative oligomers are the major cytotoxic species in tissue culture. Proc. Natl. Acad. Sci. USA 101, 2817–2822.
[10] Bucciantini, M., Giannoni, E., Chiti, F., Baroni, F., Formigli, L., Zurdo, J., Taddei, N., Ramponi, G., Dobson, C.M. and Stefani, M. (2002) Inherent toxicity of aggregates implies a common mechanism for protein misfolding diseases. Nature 416, 507–511.
[11] Volles, M.J., Lee, S.J., Rochet, J.C., Shtilerman, M.D., Ding, T.T., Kessler, J.C. and Lansbury Jr., P.T. (2001) Vesicle permeabilization by protofibrillar alpha-synuclein: implications for the pathogenesis and treatment of Parkinson's disease. Biochemistry 40, 7812–7819.
[12] Ding, T.T., Lee, S.J., Rochet, J.C. and Lansbury Jr., P.T. (2002) Annular α-synuclein protofibrils are produced when spherical protofibrils are incubated in solution or bound to brain-derived membranes. Biochemistry 41, 10209–10217.
[13] Demuro, A., Mina, E., Kayed, R., Milton, S.C., Parker, I. and Glabe, C.G. (2005) Calcium dysregulation and membrane disruption as a ubiquitous neurotoxic mechanism of soluble amyloid oligomers. J. Biol. Chem. 280, 17294–17300.
[14] Wogulis, M., Wright, S., Cunningham, D., Chilcote, T., Powell, K. and Rydel, R.E. (2005) Nucleation-dependent polymerization is an essential component of amyloid-mediated neuronal cell death. J. Neurosci. 25, 1071–1080.
[15] Chamberlain, A.K., MacPhee, C.E., Zurdo, J., Morozova-Roche, L.A., Hill, H.A., Dobson, C.M. and Davis, J.J. (2000) Ultrastructural organization of amyloid fibrils by atomic force microscopy. Biophys. J. 79, 3282–3293.
[16] Bader, R., Bamford, R., Zurdo, J., Luisi, B.F. and Dobson, C.M. (2006) Probing the mechanism of amyloidogenesis through a tandem repeat of the PI3-SH3 domain suggests a generic model for protein aggregation and fibril formation. J. Mol. Biol. 356, 189–208.
[17] Fedorov, A.N., Dolgikh, D.A., Chemeris, V.V., Chernov, B.K., Finkelstein, A.V., Schulga, A.A., Alakhov, Y.B., Kirpichnikov, M.P. and Ptitsyn, O.B. (1992) De novo design, synthesis and study of albebetin, a polypeptide with a predetermined three-dimensional structure. Probing the structure at the nanogram level. J. Mol. Biol. 225, 927–931.
[18] Dolgikh, D.A., Uversky, V.N., Gabrielian, A.E., Chemeris, V.V., Fedorov, A.N., Navolotskaya, E.V., Zav'yalov, V.P. and Kirpichnikov, M.P. (1996) The de novo protein with grafted biological function: transferring of interferon blast-transforming activity to albebetin. Protein Eng. 9, 195–201.
[19] Aphasizheva, I.Y., Dolgikh, D.A., Abdullaev, Z.K., Uversky, V.N., Kirpichnikov, M.P. and Ptitsyn, O.B. (1998) Can grafting of an octapeptide improve the structure of a de novo protein? FEBS Lett. 425, 101–104.
[20] Bocharova, O.V., Moshkovskii, S.A., Chertikova, R.V., Abdullaev, Z.K., Kolesanova, E.F., Dolgikh, D.A. and Kirpichnikov, M.P. (2002) Introduction of biologically active fragments of interferon-α_2 and insulin into the artificial protein albebetin affects immunogenicity of the final construct. Mol. Biol. 6, 84–90.
[21] Morozova-Roche, L.A., Zamotin, V., Malisauskas, M., Ohman, A., Chertkova, R., Lavrikova, M.A., Kostanyan, I.A., Dolgikh, D.A. and Kirpichnikov, M.P. (2004) Fibrillation of carrier protein albebetin and its biologically active constructs. Multiple oligomeric intermediates and pathways. Biochemistry 43, 9610–9619.
[22] Levine, H. (1995) Thioflavine-T interaction with amyloid β-sheet structures. Amyloid 2, 1–6.
[23] Klunk, W.E., Pettegrew, J.W. and Abraham, D.J. (1989) Two simple methods for quantifying low-affinity dye-substrate binding. J. Histochem. Cytochem. 37, 1273–1281.

[24] Schneider, S.W., Larmer, J., Henderson, R.M. and Oberleithner, H. (1998) Molecular weights of individual proteins correlate with molecular volumes measured by atomic force microscopy. Pflug. Arch. 435, 362–367.
[25] Geisse, N.A., Wasle, B., Saslowsky, D.E., Henderson, R.M. and Edwardson, J.M. (2002) Syncollin homo-oligomers associate with lipid bilayers in the form of doughnut-shaped structures. J. Membr. Biol. 189, 83–92.
[26] Serio, T.R., Cashikar, A.G., Kowal, A.S., Sawicki, G.J., Moslehi, J.J., Serpell, L., Arnsdorf, M.F. and Lindquist, S.L. (2000) Nucleated conformational conversion and the replication of conformational information by a prion determinant. Science 289, 1317–1321.
[27] Kelly, J.W. (2000) Mechanisms of amyloidogenesis. Nat. Struct. Biol. 10, 824–826.
[28] Modler, A.J., Gast, K., Lutsch, G. and Damaschun, G. (2003) Assembly of amyloid protofibrils via critical oligomers-a novel pathway of amyloid formation. J. Mol. Biol. 325, 135–148.
[29] Harper, J.D. and Lansbury Jr., P.T. (1997) Models of amyloid seeding in Alzheimer's disease and scrapie: mechanistic truths and physiological consequences of the time-dependent solubility of amyloid proteins. Annu. Rev. Biochem. 66, 385–407.
[30] Ahmad, A., Uversky, V.N., Hong, D. and Fink, A.L. (2005) Early events in the fibrillation of monomeric insulin. J. Biol. Chem. 280, 42669–42675.
[31] Plakoutsi, G., Bemporad, F., Calamai, M., Taddei, N., Dobson, C.M. and Chiti, F. (2005) Evidence for a mechanism of amyloid formation involving molecular reorganisation within native-like precursor aggregates. J. Mol. Biol. 351, 910–922.
[32] Blanchard, B.J., Chen, A., Rozeboom, L.M., Stafford, K.A., Weigele, P. and Ingram, V.M. (2004) Efficient reversal of Alzheimer's disease fibril formation and elimination of neurotoxicity by a small molecule. Proc. Natl. Acad. Sci. USA 101, 14326–14332.
[33] Inaba, S., Okada, T., Konakahara, T. and Kodaka, M. (2005) Specific binding of amyloid-beta-protein to IMR-32 neuroblastoma cell membrane. J. Pept. Res. 65, 485–490.